Letter

Quadrupole moments and their interactions in the triangular lattice antiferromagnet FeI_2

Gang Chen

International Center for Quantum Materials, School of Physics, Peking University, Beijing 100871, China and Department of Physics and HKU-UCAS Joint Institute for Theoretical and Computational Physics at Hong Kong, The University of Hong Kong, Hong Kong, China

(Received 5 July 2023; accepted 29 August 2023; published 25 September 2023)

Motivated by the recent experiments on the triangular lattice antiferromagnet FeI_2, we consider the presence of the quadrupole moments and their interactions between the spin-orbital-entangled local moments. In addition to the anisotropic pairwise interaction between the local moments, the interaction between the quadrupole moment arises from the interaction of the orbital occupation configurations. This is argued primarily from the time-reversal symmetry and the different orbital configurations via their exchange paths. We discuss the implication of these interactions and expect this result to be complementary to the existing works in this system and other systems alike.

DOI: 10.1103/PhysRevResearch.5.L032042

Quantum many-body systems with a large local and active Hilbert space have attracted significant attention in the recent years [1]. These include the well-known Sachdev-Ye-Kitaev non-Fermi liquid model with a large number of interacting Majorana fermions [2], the Kondo-latticelike models for intermetallics with both local moments and itinerant electrons [3], the spin-orbital-coupled Mott insulators [4], even the weak Mott insulators with active charge and spin degrees of freedom [5,6], and so on. In these systems, there often exist a large number of degrees of freedom in the local Hilbert space. These degrees of freedom are sometimes of the same character, and more commonly, they are of quite distinct characters with very different physical properties. For the latter case, their differences may help people to clarify their self and mutual interactions as well as the probing of their properties in the actual experiments. For example, in the intermetallic systems with the description of the Kondo-latticelike models, the local moments could be well modeled as the spins and probed by usual magnetic measurements such as neutron scattering, while the itinerant electrons are more appropriately described by the Landau quasiparticles in the model setting and probed by the angle-resolved photon emission, electric transports, etc. For the case of the spin-orbital-coupled Mott insulators that are of interest in this work, the distinct characters of the spin and the orbital can actually make many interesting differences in the understanding of the candidate quantum materials.

The distinct characters between the spin and the orbital degrees of freedom have already been adopted in many early works in the field. The spin interaction without the involvement of the orbitals does not usually carry any anisotropy. With the intrinsic orientation dependence, the orbitals bring the spatial anisotropy into the model. One representative example of such models is the well-known Kugel-Khomskii spin-orbital exchange model [1,7]. Upon the spin-orbital entanglement due to the strong spin-orbit coupling, the resulting effective spin models develop both the spatial anisotropy and the effective-spin-space anisotropy [8–10]. These models have played an important role in Kitaev magnets [9], pyrochlore spin ice materials [11–13], iridates, osmates [14], rare-earth triangular lattice magnets [15–17], and even many late $3d$ transition metal compounds such as cobalts and vanadates [18–20]. In this work, we are inspired by the recent work [21] on the triangular lattice antiferromagnet FeI_2 and attempt to understand the interactions of spin and orbital degrees of freedom.

In FeI_2, the Fe^{2+} ion is located in an approximately octahedral environment. Roughly, the orbitals are separated into the upper e_g and the lower t_{2g} orbitals, and the electron occupation configuration is shown in Fig. 1. Unlike the tetrahedral environment in the diamond lattice antiferromagnet $FeSc_2S_4$, the upper e_g orbitals are half-filled without any orbital degeneracy. The lower t_{2g} are filled with four electrons. In the case of the orbital degeneracy in the t_{2g} manifold, the orbital degrees of freedom are active, and the spin-orbit coupling plays a crucial role at the linear order. Even though the orbital degeneracy is actually lifted by the nonperfect octahedral environment, if the orbital separation is not large enough compared to the spin-orbit coupling, the spin-orbit coupling is still able to entangle the spin and orbital degrees of freedom here. From the Hund's coupling, the total spin is $S = 2$. The triply degenerate t_{2g} orbitals provide an effective orbital angular momentum $L = 1$. The spin-orbit coupling entangles them together and leads to an effective spin moment $\boldsymbol{J}$ with $J = 1$. In the modeling of Ref. [21], the orbital character of the moment $\boldsymbol{J}$ has already been considered, and the anisotropic effective spin interaction was obtained by considering the symmetry operation on the local moments [16,21]. Since the effective local moment is not a spin-1/2 moment, the local Hilbert space is a bit large,

Published by the American Physical Society under the terms of the Creative Commons Attribution 4.0 International license. Further distribution of this work must maintain attribution to the author(s) and the published article's title, journal citation, and DOI.

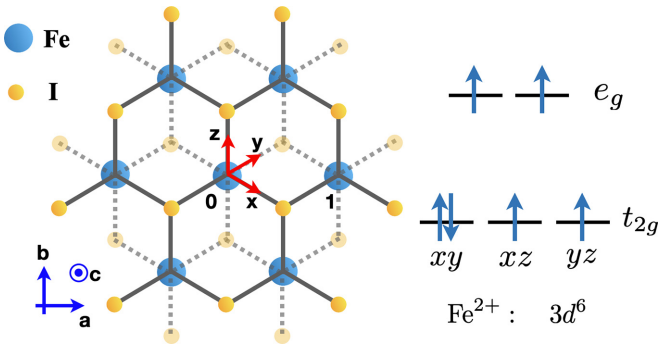

FIG. 1. The left is the lattice structure with atomic positions of FeI_2. The bright (light) yellow spheres refer to the upper (lower) I atoms. The red axes (x, y, z) refer to the spatial coordinate system for the orbitals, and the blue axes (a, b, c) refer to the coordinate system for the spin $\boldsymbol{S}$, the orbital angular moment $\boldsymbol{L}$, and the effective spin moment $\boldsymbol{J}$. The right is the electron configuration for the Fe^{2+} ion under the perfect octahedral environment in FeI_2. The orbital configuration in this plot is referred to as the XY orbital occupation.

and the spin-orbital entanglement allows the system to more effectively access this large local Hilbert space [1].

Without the careful derivation of the actual model, one can make some progress by the microscopic and the symmetry analysis. We will take this approach and then perform the calculation for the effective model. First of all, the effective model is obtained from a bit more parent model with the following form

$$H = H_{\rm KK} + H_{\rm SOC} + H_{\rm ani}, \tag{1}$$

where the first term $H_{\rm KK}$ refers to the Kugel-Khomskii spin-orbital exchange with the $S = 2$ and $L = 1$ moment, the second term $H_{\rm SOC}$ is the atomic spin-orbit coupling with the form of $\sum_i \lambda \boldsymbol{L}_i \cdot \boldsymbol{S}_i$, and the third term $H_{\rm ani}$ arises from the splitting among the t_{2g} manifold. The second and third terms provide the local onsite Hamiltonian that determines the structure of the local moment. $H_{\rm SOC}$ favors a $J = |S - L| = 1$ local moment, and $H_{\rm ani}$ becomes the single-ion anisotropy for the J representation. In the spirit of the degenerate perturbation theory, $H_{\rm KK}$ is then projected onto the degenerate manifold of the $J = 1$ states on each lattice site, and reduced to the effective spin model. Since the Kugel-Khomskii spin-orbital exchange model is usually a bit complicated, we here provide a physical understanding before performing the above procedure.

First of all, there exist eight different Hermitian operators for the $J = 1$ local moment. Among them, three are simple dipole moments, i.e., J^μ $(\mu = a, b, c)$, and five quadrupole moments with

$$Q^{3c^2} = \frac{1}{\sqrt{3}}[3(J^c)^2 - \boldsymbol{J}^2], \tag{2}$$

$$Q^{a^2b^2} = (J^a)^2 - (J^b)^2, \tag{3}$$

$$Q^{ab} = \frac{1}{2}(J^aJ^b + J^bJ^a), \tag{4}$$

$$Q^{ac} = \frac{1}{2}(J^aJ^c + J^cJ^a), \tag{5}$$

$$Q^{bc} = \frac{1}{2}(J^bJ^c + J^cJ^b). \tag{6}$$

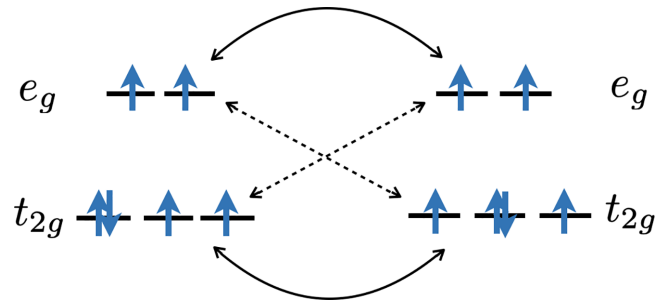

FIG. 2. The classification of the exchange process according to the manifold of the orbitals between two sites. The solid (dashed) arrows refer to the homo-orbital (hetero-orbital) exchange processes for the electrons from the identical (different) orbital manifolds.

The single-ion anisotropy $(J_i^c)^2$ can be thought of as an onsite polarization term for the quadrupole moment Q^{3c^2}. Because the quadrupole moments involve the product to two J^μ operators, they are even under time reversal symmetry. The dipole moments, however, are odd under time reversal symmetry. The distinction between the quadrupole and dipole moments may be cast as an example of magnetic moment fragmentation [22,23].

The usual pairwise spin interaction, that is obtained by the symmetry analysis, often includes the interaction between the dipole moments, and does not include the quadrupole moments. To illustrate the origin of these complicated interactions, we here return to the microscopic exchange model. Unlike the above separation of the degrees of freedom into the spin part with $S = 2$ and the orbital part with $L = 1$, we now separate the local moment from the upper e_g one and the lower t_{2g} one. The upper e_g manifold provides a spin $S_{e_g} = 1$ moment, while the lower t_{2g} manifold provides a spin $S_{t_{2g}} = 1$ and an orbital angular moment $L = 1$ with an active spin-orbit coupling. The e_g spin and the t_{2g} spin are then coupled with the ferromagnetic Hund's coupling, forming the total spin with $S = 2$. In this picture, the local Hamiltonian is given as

$$\sum_i \left[\bar{\lambda}\boldsymbol{S}_{i,t_{2g}} \cdot \boldsymbol{L}_i - J_H \boldsymbol{S}_{i,t_{2g}} \cdot \boldsymbol{S}_{i,e_g}\right] + H_{\rm ani}, \tag{7}$$

where J_H is the Hund's coupling, and $\bar{\lambda}$ is related to the λ in Eq. (1) when $\boldsymbol{S}_{i,t_{2g}}$ is reduced to the total spin $\boldsymbol{S}_i$ as $\boldsymbol{S}_{i,t_{2g}} \to \boldsymbol{S}_i/2$ after being symmetrized with $\boldsymbol{S}_{i,e_g}$. As it is equivalent to the previous discussion, this local Hamiltonian also gives the $J = 1$ spin-orbit-entangled local moment.

In the exchange of the electrons with both spin and orbital flavors for the Kugel-Khomskii model, one can classify the exchange process according to the orbital manifolds of the relevant electrons. This is depicted in Fig. 2. One can make a couple interesting observations and simplify the Kugel-Khomskii exchange model, which we explain below.

For the homo-orbital exchange process for the electrons from the upper e_g orbitals, since the orbital sector is quenched for the e_g orbital filling, this exchange process will simply give rise to the Heisenberg model in the form of

$$\sim J_1 \boldsymbol{S}_{i,e_g} \cdot \boldsymbol{S}_{j,e_g}. \tag{8}$$

This interaction, after projecting onto the $J = 1$ local moment manifold, will lead to the pairwise interaction between the dipole moments.

For the hetero-orbital exchange process between the electrons from the upper e_g and lower t_{2g} (see the dashed line in Fig. 2), the orbitals from the t_{2g} manifold become active and contribute to the exchange interaction. The site that contributes the e_g electrons, however, does not carry an active orbital information. Thus, the resulting exchange interaction should be of the following form

$$\sim J_2\big[\boldsymbol{S}_{i,e_g}\cdot\mathcal{O}_j+\mathcal{O}_i\cdot\boldsymbol{S}_{j,e_g}\big], \tag{9}$$

where $\mathcal{O}_j$ is a complicated operator that involves both $\boldsymbol{S}_{j,t_{2g}}$ and the orbital moment $\boldsymbol{L}_j$. Due to the time reversal symmetry, the operator $\mathcal{O}_j$ should be odd under time reversal. Moreover, even if the operator $\mathcal{O}_j$ may involve the operator like iQ_j^μ (with Q_j^μ as one of the quadrupole moments) when it is projected to the $J = 1$ manifold, the interaction between the dipole moment and the quadrupole moment should cancel out eventually by the hermiticity condition. Thus, despite involving the complicated $\mathcal{O}_j$ operator, Eq. (9) should also be reduced to the pairwise interaction between the dipole moments J^μ after projecting onto the $J = 1$ local moment manifold.

For the homo-orbital exchange process between the lower t_{2g} manifold, both the spins and the orbitals are involved. There are two types of operators that are involved in this exchange interaction. One type of operators is odd in $S_{t_{2g}}$ or L, such as $S^\mu_{i,t_{2g}}$ and $S^\mu_{i,t_{2g}}L^\alpha_iL^\beta_i$. These operators are labeled as $\mathcal{O}$. The exchange interaction between these $\mathcal{O}$ operators should be mostly reduced to the pairwise interaction between the dipole moments J^μ after projecting onto the $J = 1$ local moment manifold. Since $\mathcal{O}$ could be related to the quadrupole moment as iQ^μ, there can still exist some part of the interaction that becomes the quadrupole-quadrupole interaction. This requires a careful calculation. The other type of operators is even in L, such as $L^\alpha_iL^\beta_i$. These operators are labeled as $\mathcal{N}$. Due to this even property under the time reversal, the exchange interaction between these $\mathcal{N}$ operators should be mostly reduced to constant and/or the interaction between the quadrupole moments Q's. Again, since $\mathcal{N}$ could be related to the dipole moment as iJ^μ, some part of the interaction could become the interaction between the dipole moments. Thus, to obtain the interaction between the quadrupole moments in this system, one essentially needs to keep track of the exchange interaction from the homo-orbital exchange process between the lower t_{2g} manifold for both $\mathcal{O}$-$\mathcal{O}$ and $\mathcal{N}$-$\mathcal{N}$ interactions.

After the above classification and simplification, one can now focus on the exchange process between the t_{2g} electrons. This exchange process will be identical to the one for the d^4 electron configurations, or equivalently, the d^2 hole configurations on the t_{2g} manifold. We single out the bond between the Fe site 0 and the Fe site 1 in Fig. 1, and the exchange on the other bonds can be obtained by the symmetry operation. With the assumption of the ideal geometry, the Fe-I-Fe exchange path is 90 degrees. Since here we are dealing with $3d$ electrons, we consider the indirect superexchange path via the intermediate I atoms. In principle, there could be a weak direct Fe-Fe exchange, for example, via the xy orbitals from the site 0 and the site 1 in Fig. 3. For the indirect exchange path in Fig. 3, there are two relevant hopping processes. One is the d_{yz}-p_z-d_{xz} from Fe-0 to Fe-1 via the upper I atom as we have depicted in Fig. 3. The other is the d_{xz}-p_z-d_{yz} from Fe-0 to Fe-1 via the lower I atom.

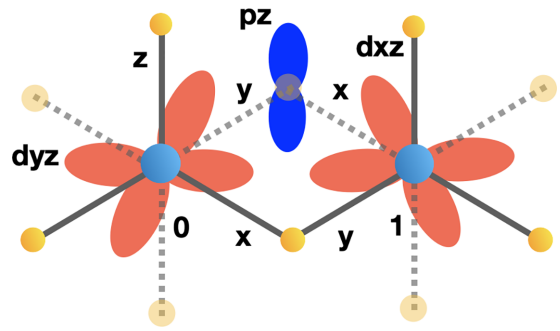

FIG. 3. The Fe-I-Fe superexchange path. In the plot, the relevant orbitals are the d_{yz} orbital at Fe-0, the p_z orbital at the intermediate I, and the d_{xz} orbital at Fe-1. Likewise, along the equivalent path via the other I atom, the relevant orbitals are the d_{xz} orbital at Fe-0, the p_z orbital at the intermediate I, and the d_{yz} orbital at Fe-1.

Since the exchange of the t_{2g} manifolds is equivalent to the one for the d^4 Mott insulators, one can actually use the existing results for the superexchange interaction [24]. Following Ref. [24], we obtain the exchange interaction for the Fe-0 and the Fe-1 that is then given as

$$\begin{aligned}H_{t_{2g},0\leftrightarrow 1} = J_{\mathrm{KK}}\big[&\big(\boldsymbol{S}_{t_{2g},0}\cdot\boldsymbol{S}_{t_{2g},1}+1\big)\big[\big(L^x_0L^y_1\big)^2+\big(L^y_0L^x_1\big)^2\\&+L^x_0L^y_0L^x_1L^y_1+L^y_0L^x_0L^y_1L^x_1\big]+\big(L^z_0\big)^2+\big(L^z_1\big)^2\big],\end{aligned} \tag{10}$$

where the components of $\boldsymbol{L}$ are defined in the xyz coordinates in Fig. 1 and Fig. 3. Again, this interaction is obtained by ignoring the direct hopping process between the xy orbitals. The Hubbard interaction is assumed to be dominant compared to the spin-orbit coupling and the Hund's coupling such that the correction from the Hund's coupling in Eq. (10) is not considered [24]. The $(L^z)^2$ term in Eq. (10), after being added with the similar terms from the symmetry equivalent bonds, will become constant, and thus can be neglected. Following our previous reasoning, the $\mathcal{O}$-$\mathcal{O}$ interaction is identified as

$$\begin{aligned}J_{\mathrm{KK}}\big(\boldsymbol{S}_{t_{2g},0}\cdot\boldsymbol{S}_{t_{2g},1}\big)\big[&\big(L^x_0L^y_1\big)^2+\big(L^y_0L^x_1\big)^2\\&+L^x_0L^y_0L^x_1L^y_1+L^y_0L^x_0L^y_1L^x_1\big],\end{aligned} \tag{11}$$

and the $\mathcal{N}$-$\mathcal{N}$ interaction is identified as

$$J_{\mathrm{KK}}\big[\big(L^x_0L^y_1\big)^2+\big(L^y_0L^x_1\big)^2+L^x_0L^y_0L^x_1L^y_1+L^y_0L^x_0L^y_1L^x_1\big]. \tag{12}$$

Ignoring the single-ion anisotropy H_{ani}, one can express the local J states in terms of the spin and orbital wavefunction in the local xyz coordinate system. One then projects the above $\mathcal{O}$-$\mathcal{O}$ and $\mathcal{N}$-$\mathcal{N}$ interactions onto the J-state basis. We then proceed and establish the relationship between the operators

$\mathcal{O}$ and the projected J operators such as

$$\boldsymbol{S}(L^x)^2 = (S^xL^xL^x, S^yL^xL^x, S^zL^xL^x) \xrightarrow{P_{J=1}} \left(\frac{6}{5}J^x, \frac{9}{10}J^y, \frac{9}{10}J^z\right), \tag{13}$$

$$\boldsymbol{S}(L^y)^2 = (S^xL^yL^y, S^yL^yL^y, S^zL^yL^y) \xrightarrow{P_{J=1}} \left(\frac{9}{10}J^x, \frac{6}{5}J^y, \frac{9}{10}J^z\right), \tag{14}$$

$$\boldsymbol{S}L^xL^y = (S^xL^xL^y, S^yL^xL^y, S^zL^xL^y) \xrightarrow{P_{J=1}} \left(\frac{3}{20}J^y - \frac{3i}{10}Q^{xz}, \frac{3}{20}J^x - \frac{3i}{10}Q^{yz}, -\frac{i}{2} - \frac{i\sqrt{3}}{10}Q^{3z^2}\right), \tag{15}$$

$$\boldsymbol{S}L^yL^x = (S^xL^yL^x, S^yL^yL^x, S^zL^yL^x) \xrightarrow{P_{J=1}} \left(\frac{3}{20}J^y + \frac{3i}{10}Q^{xz}, \frac{3}{20}J^x + \frac{3i}{10}Q^{yz}, \frac{i}{2} + \frac{i\sqrt{3}}{10}Q^{3z^2}\right), \tag{16}$$

where $P_{J=1}$ refers to the projection onto the $J = 1$ manifold.

Using the above relations, we then obtain the quadrupole interaction from above $\mathcal{O}$-$\mathcal{O}$ interaction in Eq. (11) that is given as

$$-\frac{9J_{\mathrm{KK}}}{200}\left[\frac{1}{3}Q_0^{3z^2}Q_1^{3z^2} + Q_0^{xz}Q_1^{xz} + Q_0^{yz}Q_1^{yz}\right]. \tag{17}$$

Likewise, for the quadrupole interaction from above $\mathcal{N}$-$\mathcal{N}$ interaction in Eq. (12), we use the relations

$$(L^x)^2 \xrightarrow{P_{J=1}} \frac{2}{3} + \frac{1}{20}\left(-\frac{1}{\sqrt{3}}Q^{3z^2} + Q^{x^2y^2}\right), \tag{18}$$

$$(L^y)^2 \xrightarrow{P_{J=1}} \frac{2}{3} + \frac{1}{20}\left(-\frac{1}{\sqrt{3}}Q^{3z^2} - Q^{x^2y^2}\right), \tag{19}$$

$$L^xL^y \xrightarrow{P_{J=1}} \frac{1}{10}Q^{xy}, \tag{20}$$

$$L^yL^x \xrightarrow{P_{J=1}} \frac{1}{10}Q^{xy}, \tag{21}$$

and obtain

$$\frac{J_{\mathrm{KK}}}{200}\left[\frac{1}{3}Q_0^{3z^2}Q_1^{3z^2} - Q_0^{x^2y^2}Q_1^{x^2y^2} + 4Q_0^{xy}Q_1^{xy}\right]. \tag{22}$$

The summation of Eq. (17) and Eq. (22) is the total quadrupole interaction for the 01 bond. Here we have expressed the quadrupole moments in the local xyz coordinate for the simplicity of the expression. The relation between Q's in the local coordinates and the $J^{x,y,z}$ is identical to the ones for Q's in the global abc coordinates and the $J^{a,b,c}$. The relation of Q's in the local xyz coordinates and the global abc coordinates are listed as

$$Q^{3z^2} = -\frac{\sqrt{3}}{3}Q^{a^2b^2} - \frac{2\sqrt{6}}{3}Q^{bc}, \tag{23}$$

$$Q^{x^2y^2} = \frac{2\sqrt{3}}{3}Q^{ab} + \frac{2\sqrt{6}}{3}Q^{ac}, \tag{24}$$

$$Q^{xy} = -\frac{\sqrt{3}}{6}Q^{3c^2} + \frac{Q^{a^2b^2}}{3} - \frac{\sqrt{2}}{3}Q^{bc}, \tag{25}$$

$$Q^{xz} = \frac{\sqrt{3}}{6}Q^{3c^2} + \frac{Q^{a^2b^2}}{6} - \frac{Q^{ab}}{\sqrt{3}} + \frac{Q^{ac}}{\sqrt{6}} - \frac{\sqrt{2}}{6}Q^{bc}, \tag{26}$$

$$Q^{yz} = -\frac{\sqrt{3}}{6}Q^{3c^2} - \frac{Q^{a^2b^2}}{6} - \frac{Q^{ab}}{\sqrt{3}} + \frac{Q^{ac}}{\sqrt{6}} + \frac{\sqrt{2}}{6}Q^{bc}, \tag{27}$$

and the dipole moment J^μ is given as $J^a = \frac{1}{\sqrt{2}}(J^x + J^y)$, $J^b = \frac{1}{\sqrt{6}}(J^x - J^y - 2J^z)$, and $J^c = \frac{1}{\sqrt{3}}(J^x - J^y + J^z)$. This completes the derivation of the interaction between the quadrupole moment along the bond 01. For the other equivalent bonds, one can simply obtain the quadrupole interaction via the cubic permutation.

Discussion. Here we discuss the implication of the exchange interaction between the quadrupole moments for FeI_2. Clearly, the presence of the quadrupole interaction would enhance quantum fluctuations. This is because the quadrupole moment operators connect all the spin states with more-or-less similar probability and allow the system to tunnel quantum mechanically between different spin states more effectively [1]. This aspect differs from the conventional dipole moment that only changes the spin quantum number by 0 or ± 1 at one time. Thus, a system with the substantial quadrupole interaction is more likely to be more delocalized in its spin Hilbert space and favors more exotic quantum ground states, and even for an ordered state, the usual spin-wave theory should be replaced by the flavor-wave theory that takes into account of all possible channels connected by the dipole and quadrupole operators [21,25–27]. In Ref. [21], however, the authors found a reasonable agreement with the inelastic neutron scattering spectroscopy based on a model with the single-ion anisotropy and the symmetry-allowed pairwise spin interaction. It is likely that the quadrupole interaction in FeI_2 might be weak compared to the pairwise dipole interaction as the dipole interaction has more microscopic processes than the quadrupole interaction according to the discussion. Or, the quadrupole interaction does not impact the inelastic spectrum significantly in FeI_2. The single-ion anisotropy, that is an onsite polarization term of the Q^{3c^2} moment, seems to be quite large in FeI_2 [28]. This is expected from the presence of the several magnetization plateaux or steps for FeI_2 in the c direction magnetic field [29] as well as from the recent time-domain terahertz spectroscopic measurement [28]. The presence of a large single-ion anisotropy could suppress the effect of other quadrupole interactions. A more systematic analysis may need to combine both the dipole and quadrupole interactions and at the same time acquire a more quantitative input from the density-functional theory for the exchange interactions. The isostructural material NiI_2 has a fully-filled t_{2g} manifold with quenched orbitals, and the CoI_2 has a t_{2g}^5 configuration and falls into the well-known $J = 1/2$ category [30].

Our work here provides a natural scheme to understand the origin of the multipolar interaction and can be particularly useful for the multiorbital systems with distinct

and separate orbital manifolds. One relevant system would be the Co-based Kitaev materials that are under an active investigation recently. In fact, for these Co-based honeycomb Kitaev magnets, the local moment for the Co^{2+} ion with a $3d^7$ electron configuration on the octahedral environment can be understood as the combination of the spin-1 from the e_g manifold and the spin-1/2 with an orbital moment $L = 1$ from the t_{2g} manifold. The exchange interaction over there may be understood from the separation into the e_g and the t_{2g} manifolds. It seems a similar separation scheme has already been considered for the $3d^7$ cobaltates [18]. Since the local moment for Co^{2+} is an effective $J = 1/2$ moment, the resulting interaction is always dipole interaction. This scheme simply becomes a way to organize the superexchange processes, but does not seem to provide much simplification. We thus expect a more useful application to occur in systems with larger-J moments.

Acknowledgments. This work is supported by the Ministry of Science and Technology of China with Grant No. 2021YFA1400300, the National Science Foundation of China with Grant No. 92065203, and by the Research Grants Council of Hong Kong with Grant No. C7012-21GF.

[1] G. Chen and C. Wu, Mott insulators with large local Hilbert spaces in quantum materials and ultracold atoms, arXiv:2112.02630 [cond-mat.str-el].

[2] D. Chowdhury, A. Georges, O. Parcollet, and S. Sachdev, Sachdev-Ye-Kitaev models and beyond: Window into non-Fermi liquids, Rev. Mod. Phys. **94**, 035004 (2022).

[3] P. Coleman, Heavy fermions: Electrons at the edge of magnetism, in *Handbook of Magnetism and Advanced Magnetic Materials* (John Wiley & Sons, Ltd, 2007).

[4] W. Witczak-Krempa, G. Chen, Y. B. Kim, and L. Balents, Correlated Quantum Phenomena in the Strong Spin-Orbit Regime, Annu. Rev. Condens. Matter Phys. **5**, 57 (2014).

[5] S.-S. Lee and P. A. Lee, U(1) Gauge Theory of the Hubbard Model: Spin Liquid States and Possible Application to κ-$(BEDT\text{-}TTF)_2Cu_2(CN)_3$, Phys. Rev. Lett. **95**, 036403 (2005).

[6] T. Senthil, Theory of a continuous Mott transition in two dimensions, Phys. Rev. B **78**, 045109 (2008).

[7] K. I. Kugel' and D. I. Khomskĭ, The Jahn-Teller effect and magnetism: transition metal compounds, Soviet Physics Uspekhi **25**, 231 (1982).

[8] G. Chen and L. Balents, Spin-orbit effects in $Na_4Ir_3O_8$: A hyper-kagome lattice antiferromagnet, Phys. Rev. B **78**, 094403 (2008).

[9] G. Jackeli and G. Khaliullin, Mott Insulators in the Strong Spin-Orbit Coupling Limit: From Heisenberg to a Quantum Compass and Kitaev Models, Phys. Rev. Lett. **102**, 017205 (2009).

[10] G. Chen, R. Pereira, and L. Balents, Exotic phases induced by strong spin-orbit coupling in ordered double perovskites, Phys. Rev. B **82**, 174440 (2010).

[11] S. Onoda and Y. Tanaka, Quantum Melting of Spin Ice: Emergent Cooperative Quadrupole and Chirality, Phys. Rev. Lett. **105**, 047201 (2010).

[12] Y.-P. Huang, G. Chen, and M. Hermele, Quantum Spin Ices and Topological Phases from Dipolar-Octupolar Doublets on the Pyrochlore Lattice, Phys. Rev. Lett. **112**, 167203 (2014).

[13] H. R. Molavian, M. J. P. Gingras, and B. Canals, Dynamically Induced Frustration as a Route to a Quantum Spin Ice State in $Tb_2Ti_2O_7$ via Virtual Crystal Field Excitations and Quantum Many-Body Effects, Phys. Rev. Lett. **98**, 157204 (2007).

[14] G. Chen and L. Balents, Spin-orbit coupling in d^2 ordered double perovskites, Phys. Rev. B **84**, 094420 (2011).

[15] Y. Li, G. Chen, W. Tong, L. Pi, J. Liu, Z. Yang, X. Wang, and Q. Zhang, Rare-Earth Triangular Lattice Spin Liquid: A Single-Crystal Study of $YbMgGaO_4$, Phys. Rev. Lett. **115**, 167203 (2015).

[16] Y.-D. Li, X. Wang, and G. Chen, Anisotropic spin model of strong spin-orbit-coupled triangular antiferromagnets, Phys. Rev. B **94**, 035107 (2016).

[17] Y.-D. Li, Y.-M. Lu, and G. Chen, Spinon Fermi surface $U(1)$ spin liquid in the spin-orbit-coupled triangular-lattice Mott insulator $YbMgGaO_4$, Phys. Rev. B **96**, 054445 (2017).

[18] H. Liu and G. Khaliullin, Pseudospin exchange interactions in d^7 cobalt compounds: Possible realization of the kitaev model, Phys. Rev. B **97**, 014407 (2018).

[19] R. Sano, Y. Kato, and Y. Motome, Kitaev-Heisenberg Hamiltonian for high-spin d^7 Mott insulators, Phys. Rev. B **97**, 014408 (2018).

[20] G. Jackeli and G. Khaliullin, Magnetically Hidden Order of Kramers Doublets in d^1 Systems: Sr_2VO_4, Phys. Rev. Lett. **103**, 067205 (2009).

[21] X. Bai, S.-S. Zhang, Z. Dun, H. Zhang, Q. Huang, H. Zhou, M. B. Stone, A. I. Kolesnikov, F. Ye, C. D. Batista, and M. Mourigal, Hybridized quadrupolar excitations in the spin-anisotropic frustrated magnet FeI_2, Nat. Phys. **17**, 467 (2021).

[22] M. E. Brooks-Bartlett, S. T. Banks, L. D. C. Jaubert, A. Harman-Clarke, and P. C. W. Holdsworth, Magnetic-Moment Fragmentation and Monopole Crystallization, Phys. Rev. X **4**, 011007 (2014).

[23] O. Benton, Quantum origins of moment fragmentation in $Nd_2Zr_2O_7$, Phys. Rev. B **94**, 104430 (2016).

[24] G. Khaliullin, Excitonic Magnetism in Van Vleck–type d^4 Mott Insulators, Phys. Rev. Lett. **111**, 197201 (2013).

[25] F.-Y. Li and G. Chen, Competing phases and topological excitations of spin-1 pyrochlore antiferromagnets, Phys. Rev. B **98**, 045109 (2018).

[26] F.-Y. Li and G. Chen, Spin-orbital entanglement in d^8 mott insulators: Possible excitonic magnetism in diamond lattice antiferromagnets, Phys. Rev. B **100**, 045103 (2019).

[27] J. Q. Liu, F.-Y. Li, G. Chen, and Z. Wang, Featureless quantum paramagnet with frustrated criticality and competing spiral magnetism on spin-1 honeycomb lattice magnet, Phys. Rev. Res. **2**, 033260 (2020).

[28] A. Legros, S.-S. Zhang, X. Bai, H. Zhang, Z. Dun, W. A. Phelan, C. D. Batista, M. Mourigal, and N. P. Armitage, Observation of 4- and 6-Magnon Bound States in the Spin-Anisotropic Frustrated Antiferromagnet FeI_2, Phys. Rev. Lett. **127**, 267201 (2021).

[29] K. Katsumata, H. A. Katori, S. Kimura, Y. Narumi, M. Hagiwara, and K. Kindo, Phase transition of a triangular lattice Ising antiferromagnet FeI_2, Phys. Rev. B **82**, 104402 (2010).

[30] T. Kurumaji, S. Seki, S. Ishiwata, H. Murakawa, Y. Kaneko, and Y. Tokura, Magnetoelectric responses induced by domain rearrangement and spin structural change in triangular-lattice helimagnets NiI_2 and CoI_2, Phys. Rev. B **87**, 014429 (2013).